

# P/M ALLOY 10 – A 700°C CAPABLE NICKEL-BASED SUPERALLOY FOR TURBINE DISK APPLICATIONS

D. Rice<sup>1</sup>, P. Kantzos<sup>1</sup>, B. Hann<sup>1</sup>, J. Neumann<sup>1</sup>, R. Helmink<sup>2</sup>

<sup>1</sup>Honeywell Aerospace 111 S. 34<sup>th</sup> St., Phoenix, Arizona, 85034, USA

<sup>2</sup>Rolls-Royce North American Technologies Inc. PO Box 7162 (X12), Indianapolis, IN 46207, USA

Keywords: P/M superalloys, microstructure, Alloy 10, heat treatment

## Abstract

The Versatile Affordable Advanced Turbine Engine (VAATE) program has been supporting the development of Alloy 10, a gas-atomized powder metal (PM) superalloy. Funding for the program was provided by U.S. Air Force Research Laboratory (AFRL). Honeywell International, Rolls Royce – Allison Advanced Development Company (AADC), and Williams International have been jointly developing Alloy 10 for small and large gas turbine engine applications. Alloy 10 is a demonstrated industry leader in high temperature creep resistance, and has been produced using production-scale equipment for high pressure turbine disk applications. To address cost issues, the VAATE Alloy 10 project evaluated the relative differences between material densified by hot isostatic pressing (as-HIP) and material produced by extrusion followed by isothermal forging. The program was completed as a series of four tasks: (i) chemistry optimization, (ii) as-HIP compaction, (iii) HIP compaction plus isothermal forging for small engine applications, and (iv) extrusion plus isothermal forging for large engine applications. This report provides the status of the program, microstructures typical of the various Alloy 10 product forms, and a summary of initial mechanical properties data.

## Introduction

In the design and optimization of a turbine disk alloy, attempts are made to balance the tensile and low-cycle fatigue (LCF) requirements of the disk bore with the creep rupture and dwell crack growth resistance of the disk rim. When developing the processing route for Alloy 10, additional attention was given to its notch sensitivity in an effort to enable an increased temperature exposure of the blade attachment slot. To achieve a balance of chemistry and mechanical properties, industry leaders have developed gas atomization processes, billet extrusion and isothermal forging capabilities, and specialized thermal mechanical processing methods.<sup>1</sup> Strength-dependent properties are typically enhanced by the solution heat treating forgings below the gamma prime solvus (i.e., subsolvus) followed by a rapid cooling scheme. This maintains a fine grain size while solutioning a sizable fraction of the  $\gamma'$ .<sup>2</sup> However, operating the disk rim at 700°C will require a microstructure optimized for time dependent properties, requiring a coarser grain size resulting from solution heat treating above the  $\gamma'$  solvus (i.e., supersolvus). Another option is to fabricate dual microstructure forgings, characterized by a fine grain bore and a coarse grain rim, such that the interface is located in a relatively benign region of the machined disk.

Alloy 10 is an argon gas-atomized powder nickel-based superalloy.<sup>3,4</sup> The alloy is vacuum induction melted (VIM) prior

to argon gas atomization. The powder is then sieved to -270 mesh (-53 micron) and loaded into mild or stainless steel containers and subsolvus HIP compacted. In the VAATE Alloy 10 program, material was characterized in two product forms (i) extruded billet plus isothermally forged disks (E+I) and (ii) as-HIP compacted right cylinders. The industry standard practice when fabricating non-contained high pressure turbine disks for propulsion applications is billet extrusion plus isothermal forging. Honeywell has an interest in as-HIP powder for turbine disk materials because of the significant cost savings and reduced lead times relative to isothermal forgings combined with a promising portfolio of mechanical properties. Applications where as-HIP powder metal turbine disks are viable include auxiliary power units.

The first task of the VAATE Alloy 10 program required optimization of the materials chemistry for sustained operation at 700°C. To address the tendency of the alloy to precipitate embrittling TCP phases, sub-scale as-HIP compacts of the alloy with chromium content varied from 11.0 % wt. to 13.5 % wt. were fabricated, supersolvus solution heat treated, gas fan cooled, and aged at 760°C for 16 hrs. Specimens machined from the sub-scale as-HIP compacts were submitted to notched/smooth combination creep rupture testing. The failed specimens were submitted for scanning electron microscopy (SEM) fractography and the presence of TCP phases and time to failure were correlated with % wt. Cr. This information was used to down-select the final chemistry of VAATE Alloy 10 to be used in the remainder of the program.

Materials evaluated in this program were processed to provide both subsolvus fine-grained disks and supersolvus coarse-grained disks. Sub-solvus as-HIP disks and isothermally forged disks were salt bath solution heat treated at  $\gamma'$  solvus minus 22°C, quenched into a salt bath, then stabilized and aged. Supersolvus as-HIP disks and isothermally forged disks were salt bath heat treated at  $\gamma'$  plus 22°C and quenched in a salt bath, then stabilized and aged. Salt bath heat treating was selected as the thermal processing route to enable rapid quenching while attempting to mitigate the risks associated with quench cracking. A rapid quench was desired to maximize the tensile properties of the material. Material was then stabilized at 871°C for 4 hrs to mitigate the risk of notch sensitivity in broach blade attachment slot.<sup>5,6</sup> The disks were then aged at 760°C for 16 hrs.

The intent of the supersolvus thermal processing route selected for Alloy 10 was to enable a disk rim operating temperature of 700°C. At such a high operating temperature, dwell fatigue crack growth life is a significant concern for all nickel-based superalloys, including 3<sup>rd</sup> generation materials like Alloy 10. To improve the dwell fatigue crack growth resistance of the material,

supersolvus heat treating methods were employed to purposefully create a serrated grain boundary microstructure.<sup>7,8</sup> The  $\gamma'$  solvus of Alloy 10 is  $1165.6C \pm 2.8C$ . The ideal microstructure that was sought was characterized by serrated grain boundary morphology, discrete  $M_{23}C_6$  carbide at grain boundaries, and complete solutioning of  $\gamma'$  phase, subsequently precipitated as a fine particle during cooling, stabilization, and aging. It was hoped that the fine gamma prime particle distribution resulting from the rapid quench from above  $\gamma'$  solvus would enable strength-dependent properties required in the bore.<sup>9,10</sup> The time-dependent properties required of the disk rim would be enabled by a coarse grain microstructure with serrated grain boundary morphology.<sup>11,12</sup> Attempts were made to address notch sensitivity in the blade attachment slot by subjecting all materials to a stabilization heat treatment at  $871^\circ C$  for 4 hrs.

### Experiments

The intent of the VAATE Alloy 10 program was to commercialize a high pressure turbine (HPT) disk material capable of sustained operation at rim temperatures in excess of  $704^\circ C$ . The initial work entailed the optimization of the alloy chemistry to mitigate the detrimental effects of topologically close packed (TCP) precipitates. Earlier work and a thermodynamic study completed using JMatPro had demonstrated that chromium additions in excess of 12 to 13 % wt. would likely yield brittle phases. To determine the optimum chemistry, as-HIP compacts of the alloy were fabricated with chromium ranging from 11.5 % wt. to 13.5 % wt., see Table 1. These materials were submitted to notched/smooth combination creep rupture testing and % wt. Cr correlated with time to failure, see Figure 1. The failed specimens were metallographically examined and the presence of TCP phases determined. Metallography of heat treated materials and test specimens remnants were completed using materials and procedures outlined herein.

**Table 1. The effect of % wt. Cr on Notch Creep Rupture Specimen Life.**

Specimen S/N	wt. % Cr	Stress (Mpa)	Temperature ( $^\circ C$ )	Hours	Location of failure	El. %	RA %
178820-1	11.5	468.8	760	4205.5	smooth	16.1	22.7
178820-2	11.5	468.8	760	4200*	--	--	--
178823-1	12.5	468.8	760	3407.3	smooth	11.1	14.4
178823-2	12.5	468.8	760	3496.5	smooth	10.2	14.4
178822-1	13.5	468.8	760	372.3	notch	--	--
178822-2	13.5	468.8	760	427.2	notch	--	--

\* test terminated at time indicated.

Creep rupture testing of Alloy 10 using combination specimens machined to incorporate a notch was completed to determine the effect of % wt. Cr on notch sensitivity, creep rupture life, and the propensity of the material to precipitate TCP phases. The test was completed in air at 468.8 MPa and  $760^\circ C$ , the  $K_t$  at the notch was 2.5. Upon completion of each test, the time to failure was recorded. Remnants of the failed specimens were sectioned at the fracture surface and analyzed using standard scanning electron microscopy (SEM) techniques. The presence of voiding, void coalescence, and intergranular cracking adjacent to the fracture surface was documented, see Figure 2. SEM x-ray dispersion spectroscopy (EDX) was used to determine the composition of needle-like particles, platelets, intergranular films, fine planar precipitates, and discrete grain boundary particles, see Figure 3. The final chemistry of Alloy 10 was based on a correlation between creep rupture life, thermal stability, and % wt. Cr.

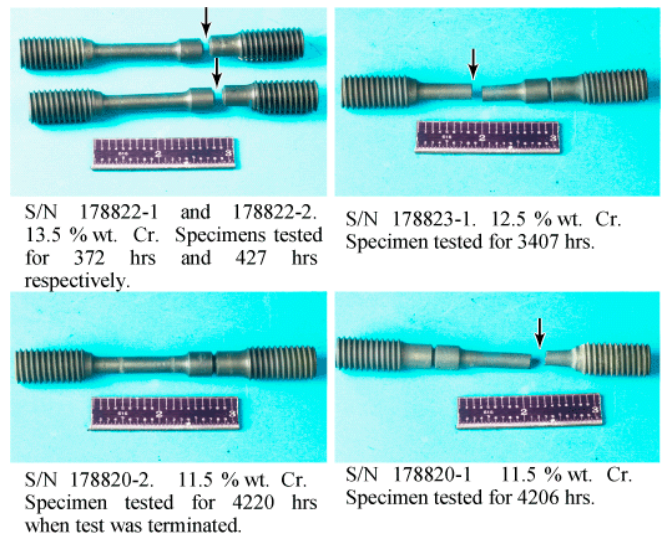


**Figure 1. Effect of % wt. Cr on Notched Creep Rupture Life and Failure Mode.**

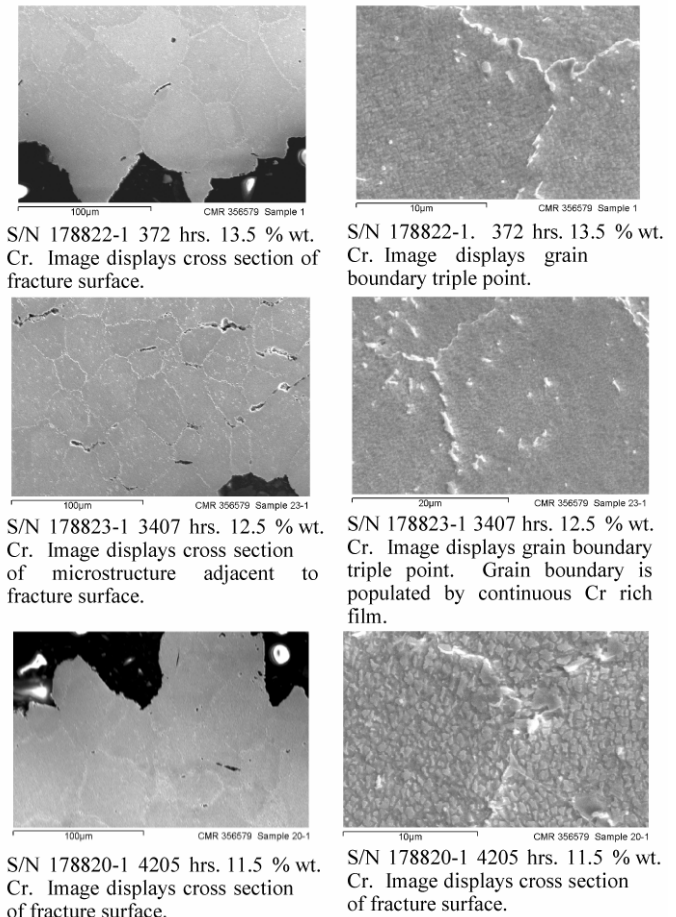


**Figure 2. Effect of % wt. Cr on Fracture Surface Morphology.**

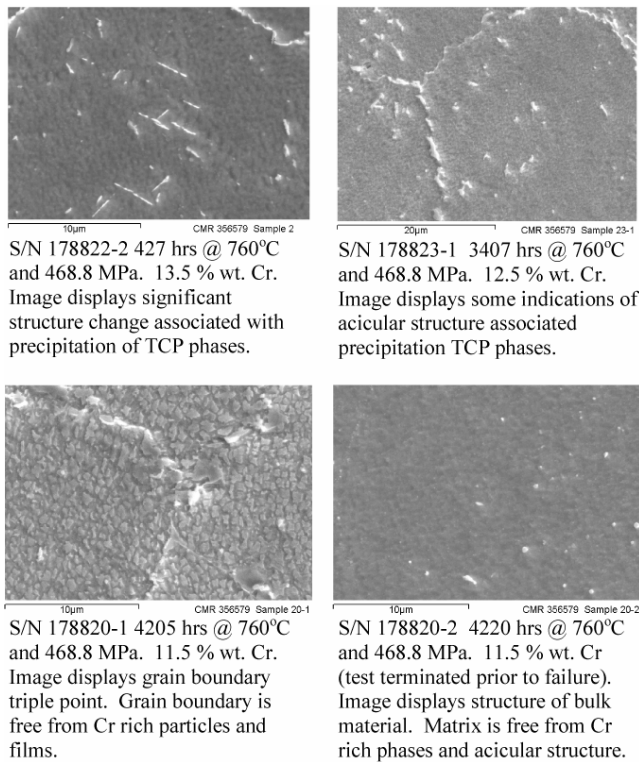


**Figure 3. Effect of % wt. Cr on Microstructure Of Creep Rupture Test Specimens.**

Heat treating of Alloy 10 is typically completed using industrial salt baths and forgings equivalent in size and mass to those used in production of small gas turbines. Subsolvus processes employed a solution at  $\gamma'$  solvus minus 22°C, quenched in to a 649°C salt bath, then stabilized and aged, see Figure 4. To understand the effect of the supersolvus heat treating method on grain boundary morphology, 28 mm diameter/3.2 mm thick coupons of Alloy 10 were heat treated in inert atmosphere at a specified temperature, slowly cooled, and quenched in air, see Figure 5. When processing the 28 mm diameter disks, the furnace control thermocouple was tack-welded to the face of the specimen and the thermal cycle recorded. Forgings subjected to a supersolvus heat treatment were solutioned at  $\gamma'$  solvus plus 22°C, quenched in to a 649°C salt bath, then stabilized and aged, see Figure 6.

Dual microstructure heat treatment of full-size gas turbine disks was completed in an air furnace. The bore of the disk was encapsulated in a nickel-alloy canister plumbed to a supply of compressed argon. Argon was flowed through the disk bore at 0.138 +/- 0.034 MPa. The set temperature on the furnace was  $\gamma'$  solvus plus 55°C. A total of six thermocouples were embedded within the thickness of the disk during the dual microstructure heat treatment. Two thermocouples were located 180° apart at the projected fine/coarse grain interface. Additional thermocouples were located 1.25 cm inboard and outboard of both interface thermocouples. The dual microstructure disks were solution heat treated until the average of the two interface thermocouples reached solvus, whereupon the disk was removed from the furnace and rapid fan cooled. Subsequently, the disks were stabilized and aged, and the microstructure documented using standard metallographic methods for PM Ni based superalloys.

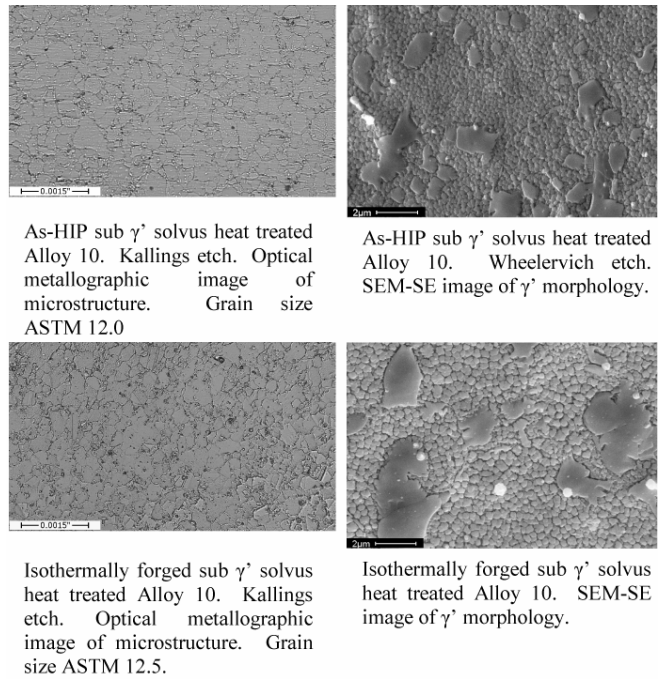


**Figure 4. Microstructure of as-HIP and Isothermally Forged Sub  $\gamma'$  Solvus Heat Treated Alloy 10.**

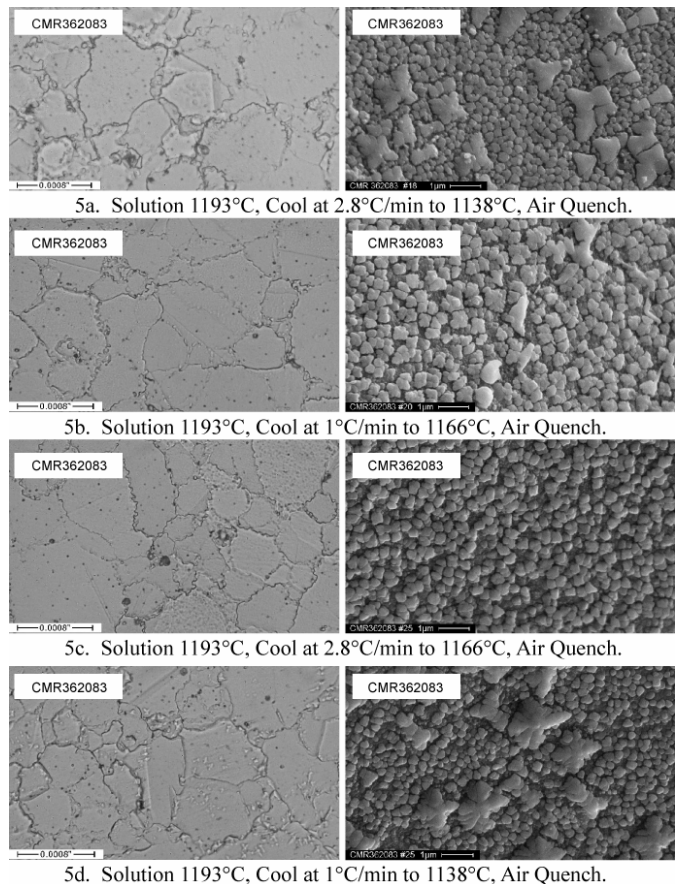


**Figure 5. Effect of Super Solvus Heat Treating on Grain Boundary Morphology.**

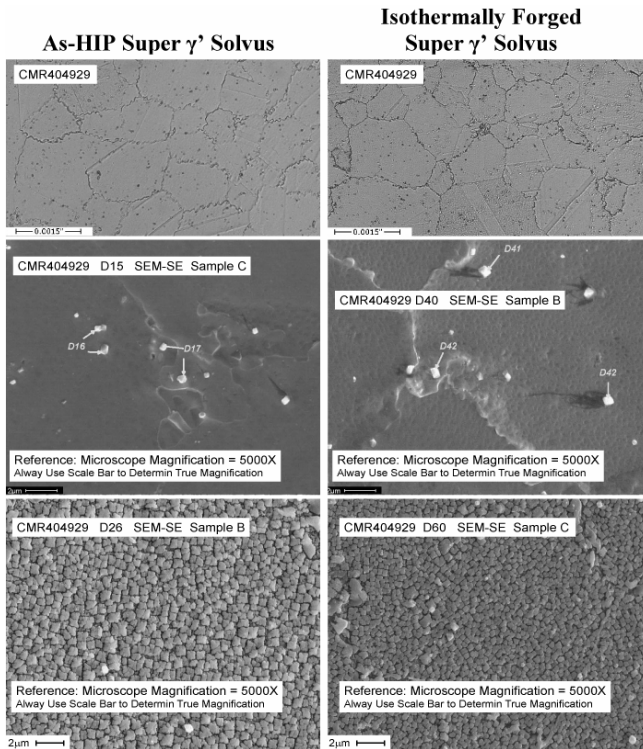


**Figure 6. Microstructure of Super  $\gamma'$  Solvus as-HIP and Isothermally Forged Disks.**

### Metallographic Method

Metallography was completed at Honeywell Aerospace in Phoenix. Optical metallography was accomplished using Kallings Etchant (5gms.  $\text{CuCl}_3$ , 100ml HCL, 100ml Methanol) and the microstructure documented. Scanning electron microscopy (SEM) was used to document the morphology and size distribution of the gamma prime phase, carbides, and grain boundaries. To document the gamma prime phase, samples were prepared using the Honeywell Wheelervich etch (94 ml Ethylene Glycol, 2 ml  $\text{HNO}_3$ , 2 ml Perchloric Acid, and 2 ml HCl). Electrolytic polish/etch parameters used were: 30 Vdc for 25 seconds and 3 Vdc for 25 seconds. To document grain boundary morphology and carbide particles samples were electrolytically etched (30 Vdc for 15 seconds only).

### Discussion

The first task of the VAATE Alloy 10 program involved optimization of the materials chemistry to enable sustained high temperature operation. To complete this task as-HIP compacts of various chemistries were fabricated, heat treated, and evaluated. The effects of % wt. Cr on creep properties and notch sensitivity were evaluated using a notched/smooth combination mechanical test specimen and an endurance test condition. Both the time to failure and the microstructure adjacent to the fracture surface of the failed specimens were correlated with the chemistry of the material. The chemistry of the billets studied varied from 11.5 % wt. Cr to 13.5 % wt. Cr. As the % wt. Cr increased the creep rupture life of the specimens decreased from 4205 hrs to a low of 372.3 hrs, see Table 1. Increasing % wt. Cr affected the failure mode of the specimens from ductile intergranular fracture

resulting from void coalescence to a brittle fracture initiated at the notch, see Figure 1. Specimens of 13.5 % wt. Cr displayed a brittle fracture surface initiating at the notch, and grain boundaries appeared to be decorated by a continuous chromium-rich film, see Figure 2. Specimens of 11.5 % wt. Cr displayed a ductile intergranular fracture surface within the gage length of the specimen, and there was significant evidence of voiding at grain boundaries adjacent to the fracture surface. When analyzed, the grain boundaries of the 11.5 % wt. Cr material displayed a morphology typical decorated by discrete  $\text{M}_{23}\text{C}_6$  carbides. An effort was undertaken to determine if any of the specimens had precipitated sigma or mu TCP phases, see Figure 3. The exact phase of the TCP particles could not be identified; however, the particles were rich in Cr. Creep rupture specimens containing 12.5 % wt. Cr and greater displayed the needle- or plate-like precipitates typical of TCP particles. These specimens were also characterized by grain boundaries decorated by a continuous chromium-rich film. Materials containing 11.5 % wt. Cr were free from TCP phases, and grain boundaries were decorated by discrete carbide particles. PM Alloy 10 is a gamma-prime strengthened nickel-based alloy containing a significant volume fraction of refractory elements typical of similar to other 3<sup>rd</sup> generation disk alloys. The higher refractory content is required to enable creep rupture properties required of higher temperature service. Additional work will be required to determine if 3<sup>rd</sup> generation disk alloys are becoming saturated in refractory elements resulting in susceptibility to TCP precipitation.

The program Tasks 2 and 3 involved the processing of as-HIP disks and isothermally forged turbine disks for small engine applications. To complete this scope of work, materials were heat treated and characterized in both the subsolvus and supersolvus heat treated conditions. Initial heat treating experiments of subsolvus material indicated that solution temperature and cooling rates were critical to properties. Based on that data, the processing route selected for PM Alloy 10 was a near-solvus solution heat treatment followed by a short delay and a salt bath quench. A stabilization thermal cycle at 871°C prior to the age cycle was introduced to provide a stress relieve and minimize the notch sensitivity of the material. The microstructure of the sub solvus heat treated material was typical for a gamma prime strengthened nickel-based alloy, see Figure 4. The grain size of the as-HIP and isothermally forged subsolvus materials was ASTM 12.0 and ASTM 12.5 respectively, see Table 2. The gamma prime morphology typically displayed residual primary gamma prime within a matrix of secondary and tertiary particles precipitated upon cooling and aging.

**Table 2. Effect of Processing and Heat Treatment on Grain Size.**

Product Form	Sub $\gamma'$ Solvus	Super $\gamma'$ Solvus
As-HIP compacted	ASTM 12.0 ALA 11.5	ASTM 7.0 ALA 5.5
Isothermal Forged	ASTM 12.5 ALA 12.0	ASTM 6.0 ALA 4.5

Super solvus heat treating was completed so as to enable the formation of a serrated grain boundary morphology, in an effort to enhance disk rim creep rupture and dwell fatigue crack growth properties at 676°C. Initial experiments investigated the effects of solution temperature, cooling rate, and quench temperature, from a supersolvus solution, on grain boundary and gamma prime morphology, see Figure 5. That work indicated that solution temperature was the most significant parameter influencing the

microstructure of the material; Cooling rate through the solvus was significant in controlling the secondary gamma prime size. A near-solvus quench yielded relatively fine serrations whereas a subsolvus quench provided coarser grain boundary serrations. The microstructure of supersolvus heat treated as-HIP and isothermally forged material was typical for a 3<sup>rd</sup> generation disk alloy, see Figure 6. The grain size for the as-HIP and isothermally forged material was ASTM 7.0 and 6.0 respectively, see Table 2.

The final task of the VAATE Alloy 10 project was to fabricate and characterize a dual microstructure turbine disk. To fabricate the dual microstructure disk, Honeywell forged and processed high pressure turbine 1<sup>st</sup> stage disks for its turbofan engine TFE731 using PM Alloy 10, see Figure 7. The disk displayed a grain size of ASTM 12.0 in its subsolvus bore and ASTM 6.5 at the rim. The grain size through the interface ranged from ASTM 12.0 to ASTM 8.5. The morphology of  $\gamma'$  particles radially along the disk cross section was typical for subsolvus and supersolvus processed material with residual primary  $\gamma'$  evident at the bore and complete solutioning of the phase at the disk rim. Additional work is on-going to determine the effect of the microstructure interface on the dwell crack growth properties of the material. The goal of this effort is to evaluate the mechanical integrity of the transition zone microstructure.

The VAATE Alloy 10 program included an extensive mechanical properties characterization of four processing variants of the material (i) as-HIP subsolvus, (ii) isothermally forged subsolvus, (iii) as-HIP supersolvus, and (iv) isothermally forged supersolvus. As stated previously, all four variants were solution heat treated in salt followed by a salt bath quench, stabilization, and age. An initial summary of properties relative to U720-Li and the NASA 3<sup>rd</sup> generation disk material LSHR is provided herein. The U720-Li was a fine-grained cast and wrought product fabricated using a controlled water quench to maximize burst properties. LSHR data was from PM material that had been extruded and isothermally forged and subsolvus heat treated to yield a fine grain size.

The tensile properties for PM Alloy 10 were determined for a variety of cooling rates based on the relative location of specimens within the forging and the size of the forging. The cooling rate from the solution temperature to approximately 870°C ranged from 30°C/min for thick sections to 100°C/min near the surface of smaller forgings, see Figure 8 displaying the tensile properties of E&I subsolvus Alloy 10 at 704°C. The tensile properties are dependant on the forging size which ultimately reflects the cooling rate. In general, the mechanical properties of PM Alloy 10 material are significantly affected by cooling rate from the solution heat treatment. Additional work is on-going to better correlate cooling rate with disk design requirements to enable optimize properties for robust turbine disk applications.

The yield strength, tensile strength, and % Elongation of Alloy 10 relative to U720-Li is provided in Figures 9, 10, and 11 respectively. The data indicates that at 648°C the yield strength of U720-Li declines below its usual utility for turbine disk applications.

Although initially lower in yield strength PM Alloy 10 crosses over the U720-Li average at 648°C and maintains its structural integrity up to 760°C in both the sub and super solvus heat treat conditions, see Figure 9. As with yield strength, cooling rate from the solution heat treatment had an effect on ultimate tensile

strength of the material, see Figure 10. Above 648°C faster cooling rates enable improved tensile strength, and above 704°C the slower cooling were sufficient to exceed the performance of U720-Li. However, the elongation of the sub solvus material was significantly affected above 648°C, see Figure 11. At the higher temperatures sub solvus heat treated material became notch sensitive.

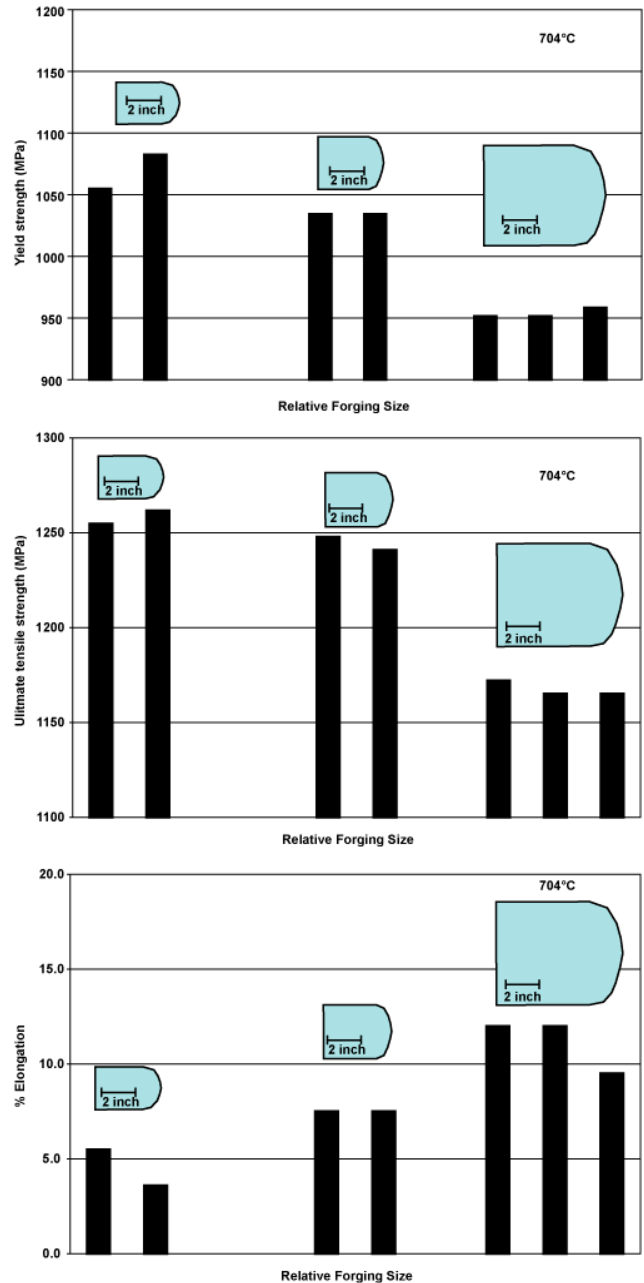


**Figure 8. Tensile Behavior of E&I Subsolvus Alloy 10 at 704°C for Various Forging Sizes, Yield Strength (Top), Ultimate Strength, (Middle) and % Elongation (Bottom).**

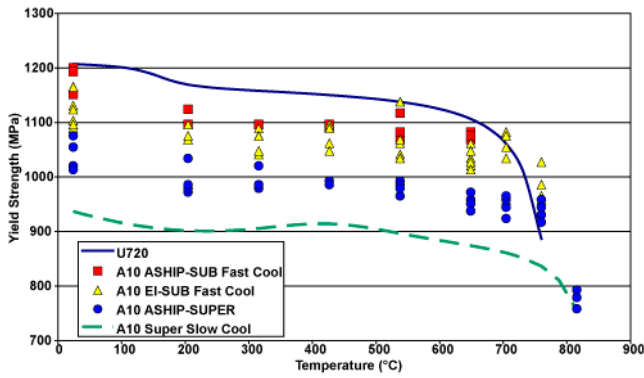


**Figure 9. Yield Strength Comparison Between U720Li and PM Alloy 10.**

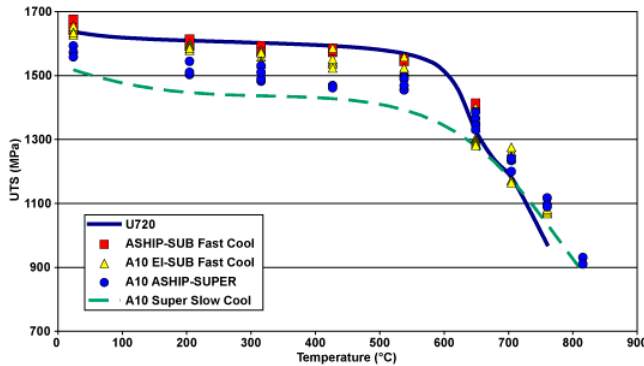


**Figure 10. Ultimate Tensile Strength Comparison Between U720Li and PM Alloy 10.**

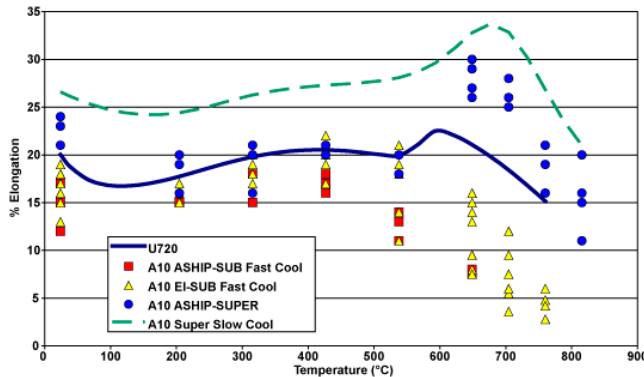


**Figure 11. Elongation Comparison Between U720Li and PM Alloy 10.**

The creep rupture time to failure between 538°C and 760°C was determined relative to U720-Li for the isothermally forged subsolvus and as-HIP super solvus material. The data indicates that PM Alloy 10 offers significantly improved creep rupture performance relative to U720-Li, see Figure 12. The subsolvus fine grained isothermally forged material out performed U720-Li across the entire test range. The as-HIP super solvus material is characterized by a uniform grain size of ASTM 7.0 +/- 0.5. The coarser microstructure enables enhanced high temperature creep rupture performance relative to fine grain material.

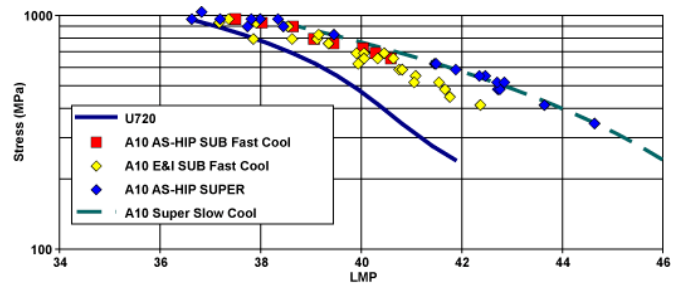


**Figure 12. Creep LMP Comparison Between U720Li and PM Alloy 10.**

The improvement to creep rupture life of super solvus heat treated material is evident in Figure 12. Honeywell employs as-HIP super solvus material as turbine disks in its auxiliary power unit applications because of its economy of fabrication and unique combination of properties.

The fatigue crack growth behavior of Alloy 10 was characterized between 427°C and 760°C. Crack growth testing was performed using a surface flaw geometry specimen. Tests were performed at constant load with R=0.05 using a triangular wave at 20 cycles per minute (CPM). Dwell tests were performed under the same conditions using a 90 sec hold at maximum load. The two principle forms of the alloy characterized were (i) isothermally forged subsolvus and (ii) as-HIP supersolvus. These two product forms are of interest because they enable a fine grain material (ASTM 12) for engine designs limited by low-cycle fatigue life and a coarse grain material (ASTM 7.0) with enhanced creep rupture and dwell fatigue resistance for engine designs limited by dwell fatigue. The relative non-dwell fatigue crack growth resistance of these two materials is shown in Figures 13 and 14. With respect to fatigue crack growth life, the coarse grain microstructure supersolvus material can offer a significant temperature advantage, as much as 100°C, in comparison to subsolvus material over the range of temperatures studied. The fatigue crack growth failure mode below 649°C was primarily transgranular for both microstructures. At 649°C and above the failure mode transitioned to predominantly intergranular for the subsolvus microstructure. For the supersolvus microstructure the transition to predominantly intergranular failure occurs at a higher temperature somewhere between 649°C and 760°C; because at 649°C, the supersolvus failure mode was still predominantly transgranular.

The effect of dwell on the crack growth behavior is shown in Figures 15 and 16. At 649°C, a 2X increase in crack growth rate is observed for both materials under dwell. In both cases, dwell is associated with an increase in intergranular failure. In the subsolvus microstructure, dwell results in completely intergranular failure. The supersolvus microstructure failure mode at 649°C still maintains some transgranular feature.

At higher temperatures, 704°C for the subsolvus material and 760°C for the supersolvus material, the corresponding increase in crack growth rate is approximately 10X. Again the supersolvus microstructure offers approximately a 50°C advantage over the subsolvus material in dwell crack growth behavior. At these temperatures, both materials exhibit fully intergranular fracture paths. Failure along prior particle boundaries was not evident in either material.

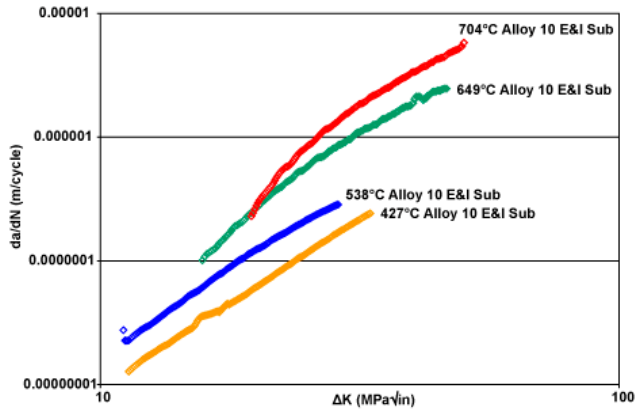


Figure 13. Fatigue Crack Growth Behavior for Sub  $\gamma'$  Solvus E&I Alloy 10.

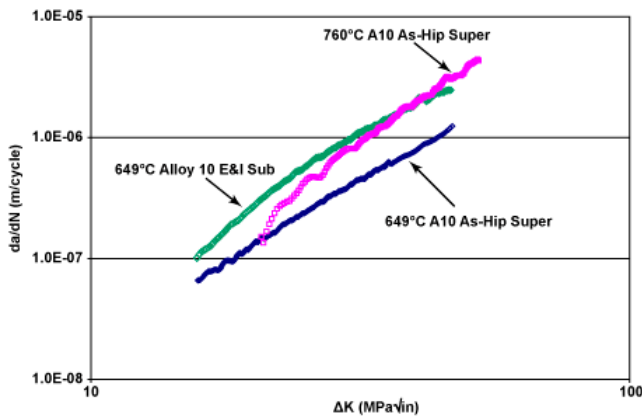


Figure 14. Fatigue Crack Growth Behavior of As-Hip Super  $\gamma'$  Solvus Alloy 10, Sub  $\gamma'$  Solvus E&I Alloy 10 as Shown at 649°C for Comparison.

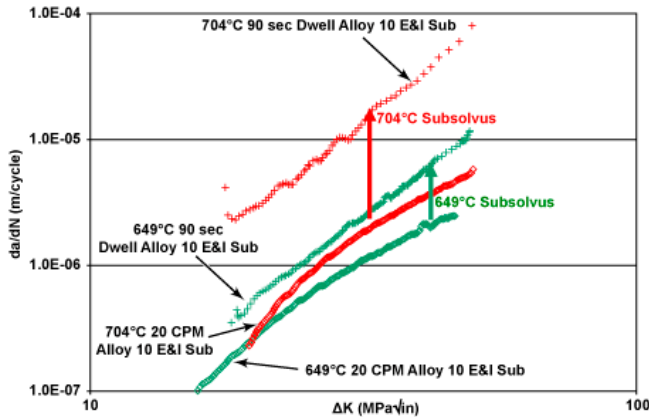


Figure 15. Alloy 10 Sub  $\gamma'$  Solvus E&I, 90 sec Dwell Fatigue Crack Growth Behavior Shown in Comparison to 20 CPM.

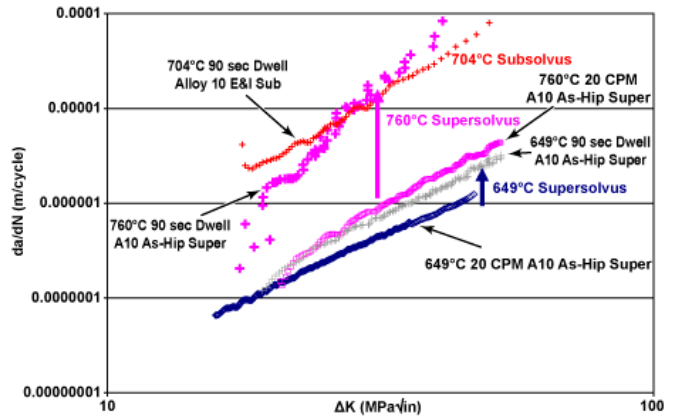


Figure 16. Alloy 10 Super  $\gamma'$  Solvus As-Hip, 90 sec Dwell Fatigue Crack Growth Behavior Shown in Comparison to 20 CPM. The Dwell Crack Growth Behavior of Sub  $\gamma'$  Solvus E&I Alloy 10 is also Shown for Comparison at 704°C.

### Conclusions

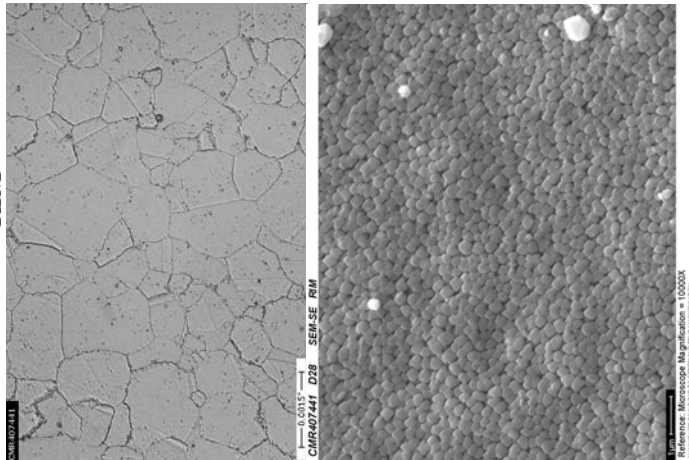
PM Alloy 10 is a promising turbine disk material enabling 700°C disk rim temperatures and increased power density for future engine applications. The alloy can be processed and heat treated in a number of variants to yield materials customized to unique applications. The chemistry has been tailored to inhibit the precipitation of TCP phases. When super  $\gamma'$  solvus heat treated the material will yield a serrated grain boundary morphology enabling enhanced resistance to creep rupture and dwell fatigue crack growth at higher operating temperature. Attempts to fabricate a dual microstructure turbine disk were also successful. When heat treated to provide a fine-grained microstructure, mechanical properties were comparable with similar materials up to approximately 649°C. Operating turbine disks at 700°C will most likely require a coarser-grained material with a unique microstructure to resistant dwell fatigue initiated failure modes. Alloy 10 has been supersolvus heat treated in salt baths and rapidly quenched to yield an interesting combination of tensile, creep rupture, and dwell fatigue crack growth properties. The VAATE Alloy 10 team from Honeywell, Rolls Royce AADC, and Williams International would like to thank the people at AFRL for their support, patience, and encouragement while completing this work.

## References

1. J. J. Schirra et. al. Effect of Microstructure (and Heat Treatment) on the 649°C Properties of Advanced P/M Superalloy Disk Materials. Superalloy 2004; The Minerals, Metals and Materials Society; 2004; edited by K. A. Green et. al. page 341 to 350.
2. J. Gayda et. al. The Effect of Dual Microstructure Heat Treatment on an Advanced Nickel Base Disk Alloy. Superalloys 2004; The Minerals, Metals and Materials Society; 2004; edited by K. A. Green et. al. page 323 to 329.
3. A. Hieber, H. Merrick, "High Temperature Powder Metallurgy Superalloy with Enhanced Fatigue and Creep Resistance" U. S. Patent 6,969,431, November 2005.
4. A. Hieber, H. Merrick, "High Temperature Powder Metallurgy Superalloy with Enhanced Fatigue and Creep Resistance" U. S. Patent 6,866,727, March 2005.
5. J. Gayda et. al. The Effect of Solution Cooling Rate on Residual Stresses in an Advanced Nickel-Base Disk Alloy. NASA/TM-2004-213081, June 2004.
6. J. Telesman et. al. Microstructural Variables Controlling Time-Dependent Crack Growth in a P/M Superalloy. Superalloy 2004; The Minerals, Metals and Materials Society; 2004; edited by K. A. Green et. al. page 215-224.
7. R. J. Mitchell et. al. Development of  $\gamma'$  Morphology in P/M Rotor Disk Alloys During Heat Treatment. Superalloys 2004; The Minerals, Metals and Materials Society; 2004; edited by K. A. Green et. al. page 361 to 370.
8. A. K. Koul and R. Thamburak. Serrated Grain Boundary Formation Potential of Ni-Based Superalloys and Its Implications. Metallurgical Transactions A. Volume 16a, January 1985 page 17.
9. A. K. Koul and G. H. Gessinger. On the Mechanism of Serrated Grain Boundary Formation in Ni-Based Superalloys. Acta Metall. Vol. 31, No. 7, pages 1061-1069; 1983.
10. J. M. Larson. Carbide Morphology in PM IN792. Metallurgical Transactions A; Volume 7A, pages 1497-1502. October 1976.
11. D. Ellis and T. Gabb. Microstructural Evaluation of KM4 and SR3 Samples Subjected to Various Heat Treatments. NASA/TM-2004-213140, August 2004.
12. J. Gayda et. al. The Effect of Heat Treatment on the Fatigue Behavior of Alloy 10. NASA/TM-2003-212473, August 2003.

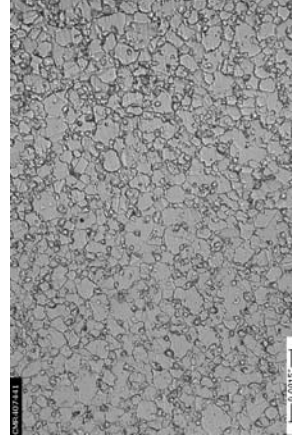
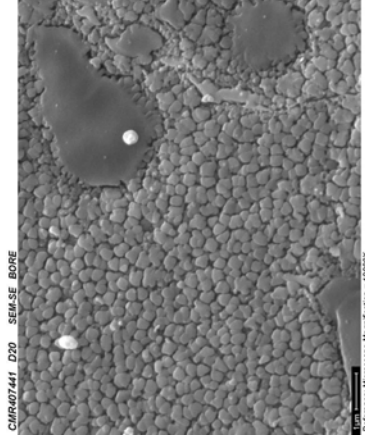
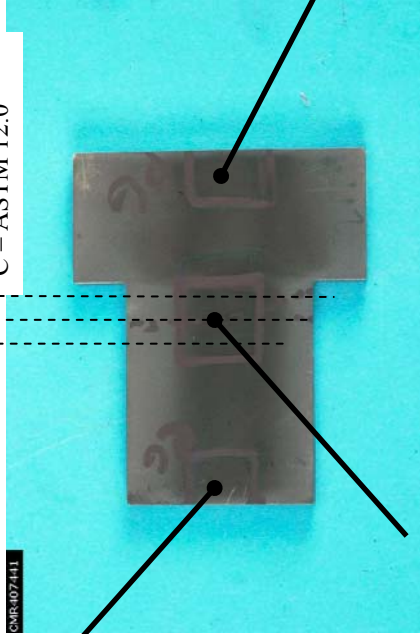


**RIM**

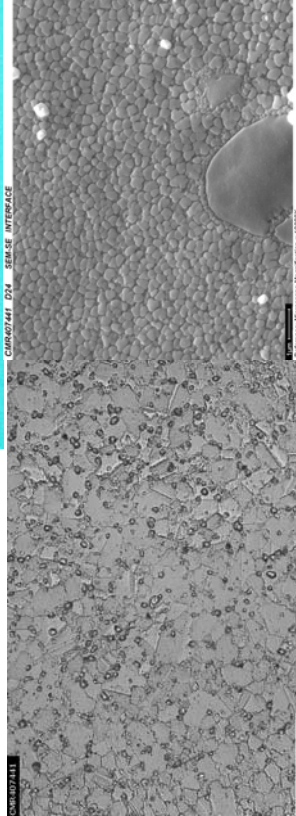


**Interface**

- A - ASTM 8.5
- B - ASTM 10.0
- C - ASTM 12.0



**BORE**



**INTERFACE**

Figure 7. PM Alloy 10 Dual Microstructure Turbine Disk.